Journal of Alloys and Compounds 654 (2016) 554–560

Contents lists available at ScienceDirect

Journal of Alloys and Compounds

journal homepage: http://www.elsevier.com/locate/jalcom

Structural stability of ultra-incompressible Mo_2B: A combined experimental and theoretical study

M. Sekar [a, *], N.V. Chandra Shekar [a], S. Appalakondaiah [b], G. Shwetha [c], G. Vaitheeswaran [b], V. Kanchana [c]

[a] Condensed Matter Physics Division, Materials Science Group, Indira Gandhi Centre for Atomic Research, Kalpakkam, 603102, Tamil Nadu, India
[b] Advanced Center of Research in High Energy Materials, University of Hyderabad, Gachibowli, Hyderabad 500 046, Telangana, India
[c] Department of Physics, Indian Institute of Technology Hyderabad, Ordinance Factory Estate, Yeddumailaram, 502 205, Telangana, India

ARTICLE INFO

Article history:
Received 10 September 2015
Accepted 14 September 2015
Available online 16 September 2015

Keywords:
Transition metal semiboride
Pressure
X-ray diffraction
Electronic structure
Structural stability
Density of states
Mo_2B

ABSTRACT

In the present work, we report a combined experiment and theoretical study on high pressure structural stability of Al_2Cu type- Mo_2B up to ~40 GPa. Experiments using rotating anode x-ray source indicate that the ground state tetragonal structure of Mo_2B (space group *I4/mcm*) to be stable up to the highest pressure studied. In addition, the experimental results were complemented by first principles density functional calculations within the projector augmented wave method. The calculated structural parameters are in excellent agreement with present experiments as well as previous reports. The estimated bulk modulus using Birch–Murnaghan equation of state from both experiment (302 GPa) and theory (310 GPa) reveals the ultra-incompressible nature of Mo_2B. The much higher bulk modulus of this semi boride as compared to elemental Mo is discussed in terms of Mo–Mo bond distance in their crystal structures. The calculated electronic structure of Mo_2B shows a strong Fermi surface nesting along P–P direction, which might also trigger lattice instability and is addressed in detail.

© 2015 Elsevier B.V. All rights reserved.

1. Introduction

Transition metal carbides (C), nitrides (N) and borides (B) are large as well as complex group of industrially relevant compounds with outstanding physical properties [1]. The combination of metals with light covalent-bond forming atoms like B, C and N often leads to materials which are not only having high melting point, but also show very low compressibility and high hardness compared with the pure metal [1]. Transition-metal (TM) semi borides (TM_2B; TM = Ti, Cr, Mn, Fe, Co, Ni and Mo) crystallize in the tetragonal Al_2Cu type structure (*I4/mcm*) [2] and most of these materials are reported as super hard materials, where the reported bulk moduli are usually higher than 200 GPa [2–5], and the crystal structures of these compounds strongly depend on the TM to B ratio. Besides this, borides show special features of short boron–boron contacts and formation of one, two, three dimensional boron networks [6]. In addition, the other quite interesting fact is that these compounds show a variety of magnetic states, where Cr_2B and Mn_2B are anti-ferromagnetic; Fe_2B and Co_2B are ferromagnetic; Ni_2B, Mo_2B and W_2B are paramagnetic [7]. The electronic structures and hyperfine field of several transition metal semi-borides were reported in literature in which the authors found a good agreement between theory and experiments [2]. The calculated enthalpy of formation for several TM_2B compounds clearly indicates that they are thermodynamically stable [8]. It is a known fact that high pressure experiments on such metal-semi borides are sparse and recently we have investigated nickel semi boride (Ni_2B) under high pressure by x-ray diffraction up to ~ 28 GPa and addressed its structural stability [3].

Nowadays, molybdenum based borides (MoB_x) have been receiving considerable interest as super hard materials (bulk moduli > 300 GPa) [9] and the prediction of crystal structure for these systems remains challenging from both experiments as well as theory. Among them, the experimental reports on Mo_2B are restricted to the refinement of the crystal structure at ambient conditions [10]. Theoretical calculations report covalent nature of Mo–Mo bond with less predominant d-orbital splitting. Apart from this, recent *ab-initio* studies using super cell approach method (within the harmonic approximation) reported that the Al_2Cu structure for Mo_2B is dynamically unstable from the phonon

---

* Corresponding author.
E-mail address: sekarm@igcar.gov.in (M. Sekar).

http://dx.doi.org/10.1016/j.jallcom.2015.09.128
0925-8388/© 2015 Elsevier B.V. All rights reserved.

dispersion calculations. Zhou et al. examined the phonon dispersion at ambient conditions and concluded that I4/*m* structure of Mo_2B has minimum energy than *I*4/*mcm* structure by examining the atomic displacements [11]. In addition to this, Aryal et al. [12] reported the mechanical, dynamical as well as thermodynamic properties of Mo_2B using density functional calculations and found an anomalous lattice instability of acoustic branch (nearly-130 cm^{-1}) at Gamma (Γ) point of phonon dispersion and conclude that instabilities arise due to the temperature effects. Beyond these, no other reports are available for this compound. Since Mo_2B is a metal, the anomalies in the phonon frequencies may originate from the electron–phonon interaction and so it is necessary to have deep understanding about conventional electronic properties as well as fermi surface topology, which is not yet reported. Therefore, it is worth to revisit the stability of Mo_2B using both experiment as well as theoretical calculations, which is the prime goal of this paper.

In this paper, we have investigated the structural stability at ambient conditions and at higher compressions of Mo_2B, up to 40 GPa using high pressure experiments. In addition to this, first principles calculations based on density functional theory have been carried out to complement the experimental results on structural properties. Also, our Fermi surface studies reveal a strong Fermi surface nesting in this compound, which might be the reason for the earlier observed structural instability and is well addressed in the present work. The rest of the paper is organized as follows: In Sec. 2 we present our experimental and theoretical methodologies, while results of experiment and theory are presented and discussed in Sec. 3. Finally, Sec. 4 concludes the present work.

2. Methodology

2.1. Experimental details

Mo_2B powder (99% pure) procured from M/s Alfa Aesar was characterized using IP based mar345dtb diffractometer and the lattice parameters at ambient were found to match with ICDD standard values (PDF card no.04-001-0962) [4]. The sample was found to be Al_2Cu type tetragonal structure (space group I4/mcm) with the lattice parameters $a = 5.549$ Å and $c = 4.733$ Å. The obtained lattice parameters were in excellent agreement with previous experiments [9] and the complex crystal structure of Mo_2B is shown in Fig. 1.

High pressure X-ray diffraction (HPXRD) studies were performed in a Mao-Bell type DAC using angle dispersive X-ray diffraction with a rotating anode x-ray generator (Rigaku-ULTRAX-18) with Mo target ($\lambda = 0.7107$ Å) in conjunction with an image plate based mar345dtb up to a pressure of ~40 GPa. The two dimensional x-ray patterns were integrated by using the program ***fit2d*** [13]. Stainless steel (SS) gaskets were preindented to a thickness of ~70 μm and a hole of diameter 200 μm was drilled at the centre of the compressed area for mounting the sample. A mixture of methanol, ethanol and water (MEW) in the volume ratio 16:3:1 was used as pressure transmitting medium. Ruby fluorescence technique was used to estimate the sample pressure.

2.2. Computational details

The first principles total energy calculations were performed within the framework of density functional theory (DFT) formalism. The structural properties as well as equation of state were examined using projector augmented wave (PAW) method as implemented in Vienna Ab-initio Simulations (VASP) Package [14]. The exchange-correlation potential of Perdew–Burke–Ernzerhof (PBE) with generalized gradient approximation (GGA) for electron–electron interactions is used [15]. To confirm the convergence of the calculations for Brillouin zone sampling, we have investigated the minimum total energies on the cutoff energy and the k-point set mesh according to the Monkhorst–Pack grid scheme [16]. Cut-off energy of 800 eV and k-point set of 12 × 12 × 12, were chosen for calculations. The convergence of the total energy is set to 1×10^{-8} eV/atom and the maximum force on the atom is 10^{-4} eV/Å. To perform the high pressure geometry optimizations (from 0 to 40 GPa with a step size of 4 GPa), variable cell method was adopted. The electronic structure calculations were performed using Full-potential Linear Augmented Plane Wave (FP-LAPW) method as implemented in WIEN2K [17] code using the GGA-PBE method. In order to perform the electronic properties calculations, we have used the optimized geometries obtained by VASP-PBE method. Throughout our calculations, we have used the $R_{MT} \times K_{max}$ value to be 8, where R_{MT} is the smallest of the muffin-tin radius, K_{max} is the plane wave cut-off energy for the expansion of wave function in the interstitial region, while the charge density was Fourier expanded up to $G_{max} = 12$. We have used 34 × 34 × 34 k-mesh with 2844 k-points in the Irreducible Brillouin Zone (IBZ) for the electronic structure calculations, and the Fermi surface calculations. Here the crystal structure and Fermi surface topologies were plotted by VESTA and XCRYSDEN software.

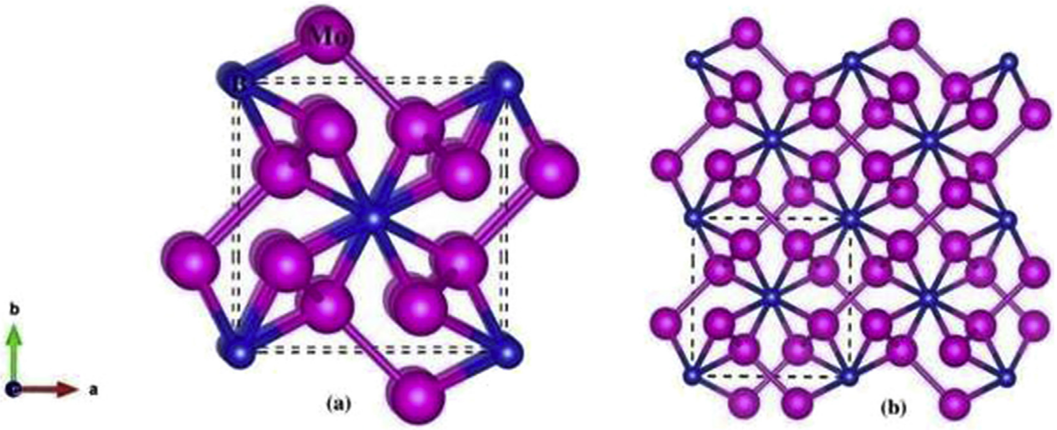

Fig. 1. (a) Crystal structure of Al_2Cu type Mo_2B, (b) Super cell of Mo_2B.

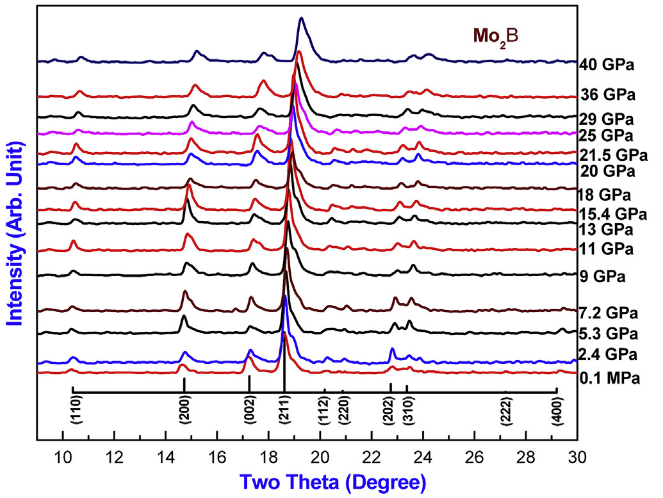

Fig. 2. HPXRD patterns of Mo_2B up to ~40 GPa obtained with a RAXRG (λ = 0.7107 Å). Ruby fluorescence was used to estimate the pressure. The stick plot is the PDF data for Mo_2B.

3. Results and discussions

3.1. Structural properties

The evolution of HPXRD patterns for Mo_2B at various pressures up to ~40 GPa are depicted in Fig. 2. From this, it is seen that the diffraction pattern is unchanged with increasing pressure up to ~40 GPa except for the systematic shift in diffraction lines caused by the decrement in lattice parameters. In addition, broadening of the diffraction peaks with increasing pressure is observed and, all the diffraction peaks (110), (200), (002), (211), (112), (220), (202), (310), and (222) could be indexed up to highest pressure investigated. The stick plot is the standard PDF data of Mo_2B [4]. This implies that I4/mcm phase of Mo_2B is stable at ambient conditions and no symmetry change was observed up to 40 GPa. In contrast to the present experiment, two recent theoretical studies [11,12] reported tetragonal Mo_2B to have large imaginary phonon frequencies concluding the dynamical instability of the I4/mcm structure at ambient conditions and the possible reason for the same will be discussed in the succeeding section. Besides this, the calculated structural properties within GGA are in excellent agreement with the present experiments as well as previous theoretical results. The ground state lattice parameters and volume obtained in the present work from both experiments and theory together with previous reports are illustrated in Table 1. From this, it is found that the calculated lattice parameter "*a*" is in agreement with present experiments and lattice constant "*c*" as well as unit cell volume is slightly overestimated by (~0.4%).

Table 1
Lattice parameters (*a*, *c*), Bulk modulus (in GPa) and its pressure derivative of I4/mcm phase Mo_2B at ambient pressure obtained by present experiment, theory and other previous reports. Here the theoretical calculations were performed within GGA-PBE method.

Parameter	Present		Others	
	Experiments	Theory	Experiments	Theory
a (Å)	5.549	5.546	5.543[9]	5.5437[11], 5.5449[12]
c (Å)	4.733	4.754	4.735[9]	4.7549[11], 4.7550[12]
V (Å^3)	145.75	146.21	145.48[9]	146.13[11], 146.20[12]
B_o (GPa)	310.0	302.8	–	–
B′	4.5	4.2	–	–

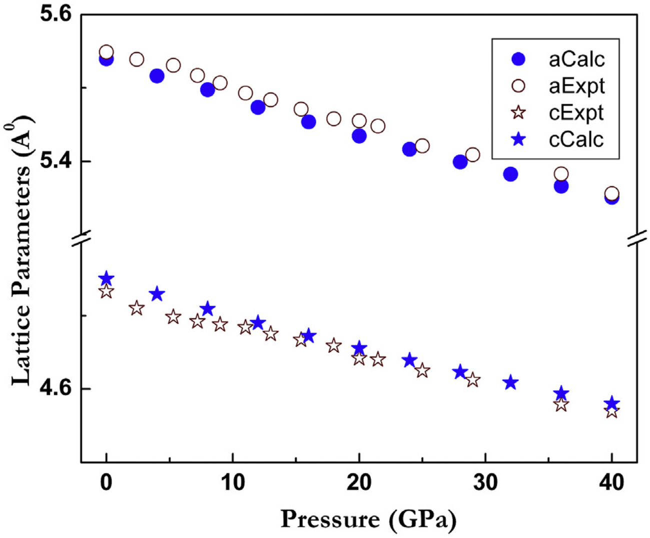

Fig. 3. Variation of lattice parameters *a* & *c*-of Mo_2B using experiment and computation.

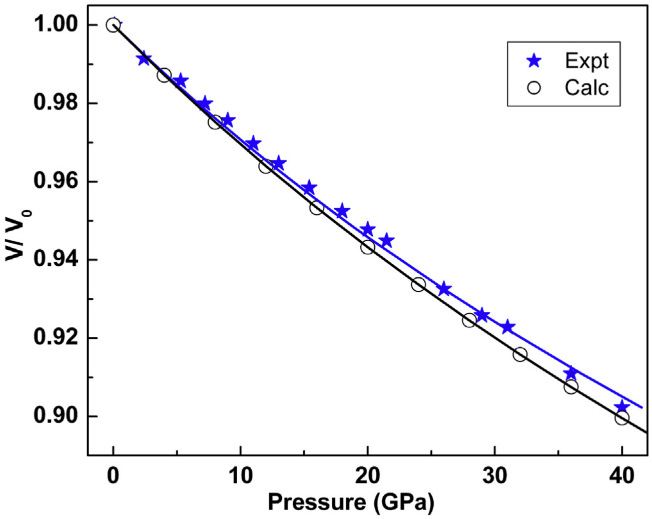

Fig. 4. P– V data of Mo_2B fitted to Birch–Murnaghan EOS for both experiment and computation.

Now, we further move to analyse the variation of lattice parameters and volume as a function of pressure up to 40 GPa. The influence of pressure on tetragonal lattice parameters (*a*, *c*) on both experimental and computed values is shown in Fig. 3. From this, it is seen that lattice parameters are continuously decreasing upon the compression and the computed results are in good agreement with present experiments by an exception of small fluctuations (~0.5%) in "*c*"-lattice parameter. In fact, present experiments were conducted at room temperature, whereas the calculated results are at T = 0 K. Apart from this, the decrement in the lattice parameters "*a*" and "*c*" are 0.193 (0.189) and 0.163 (0.170) Å respectively using experiments (theory) up to 40 GPa. This indicates that "*a*" lattice parameter is more compressible than "*c*" lattice parameter in the *I4/mcm* phase of Mo_2B structure. The variation of relative volume (V/V_0) as a function of pressure (P) is shown in Fig. 4. Similar to *c*-lattice parameter, the computed V/V_0 (filled symbols) also slightly vary with the present experiment (open symbols) and the overall agreement is good with an error of ~ (0–0.5) % throughout the pressure range. In order to calculate the bulk modulus (B_0) and its

Table 2
Shows the compounds, lattice parameters, TM- B, B— B bond length and bulk modulus for 3d, 4d, 5d TM_2B compounds, which crystallize in Al_2Cu type tetragonal structure. The data is taken from literature except for Mo_2B is the present work. The bulk modulus for Ta_2B is not available.

Compound	Structure	*a*(Å)	*c*(Å)	TM-TMdist(Å)	TM- B-dist(Å)	B—B dist(Å)	Vol/form. Unit (Å^3)	Bulk mod(GPa)
Ti_2B(3d)	Al_2Cu	6.100	4.53	2.68	2.53	2.27	42.14	218^2
Cr_2B(3d)	Al_2Cu	5.180	4.310	2.48	2.21	2.15	28.91	279^2
Mn_2B(3d)	Al_2Cu	5.148	4.208	2.43	2.19	2.10	27.88	301^2
Fe_2B(3d)	Al_2Cu	5.109	4.249	2.44	2.18	2.12	27.73	249^2
Co_2B(3d)	Al_2Cu	5.016	4.220	2.42	2.15	2.11	26.54	247^2
Ni_2B(3d)	Al_2Cu	4.99	4.24	2.43	2.14	2.12	26.43	236^3
Mo_2B(4d)	Al_2Cu	5.549(Expt)	4.733(Expt)	2.70(Expt)	2.38(Expt)	2.366(Expt)	36.43(Expt)	310(Expt) 302(Calc)
		5.5399(Calc)	4.750(Calc)	2.71(Calc)	2.38(Clac)	2.375(Clac)	36.44(Calc)	This work
Ta_2B(5d)	Al_2Cu	5.783	4.866	2.789	2.475	2.433	40.68	N/A^4
W_2B(5d)	Al_2Cu	5.580	4.772	2.711	2.39	2.37	36.77	314^7

pressure derivative (B′) of Mo_2B, we have fitted the obtained P— V data with Birch—Murnaghan equation of state for both experimental and computed results. The obtained B_0 (B′) are: 310 GPa (4.5) and 302 GPa (4.2) corresponding to both experiment and theory, where the agreement is slightly lower with an underestimation of 0.3%. It is also to be noted that the present B_0 value from theory is in reasonable agreement with the previously reported bulk modulus value of 298.6 GPa [12]. At this instance, we try to compare the obtained bulk modulus of the present compound with other transition metal-semi borides to understand the nature of hardness of Mo_2B.

Table .2 illustrates the comparison of all available TM_2B compounds (3d, 4d and 5d TM-B systems), which crystallize in Al_2Cu type structure. From this, it is observed that among the 3d semi borides, the lattice parameters, bond lengths (TM—TM, TM- B, B—B), and volume/formula unit decreases along the period, whereas bulk modulus maximizes at Mn, which could be due the half filling of the 3d orbital and short B—B bond length (2.1 Á). If we consider the variation along the Group VI A elements from Cr to W, all the lattice parameters, bond distances and bulk modulii increases systematically. In general, the compounds have bulk modulus higher than 200 GPa, indicating the super hardness. Also, among the 4d transition series starting from Y to Cd, only four elements Mo, Ru, Rh and Pd form semi borides crystallizing in different structure types (except in the case of Mo_2B).

Now, we compare the other borides of molybdenum such as MoB, MoB_2, Mo_2B_5, MoB_3 and MoB_4. Among these, MoB has the highest bulk modulus of 324 GPa and the bulk modulus has direct correlation with the electron densities of these compounds [9]. In elemental molybdenum the metallic Mo—Mo bond has a bond distance of 2.72 Å whereas in Mo_2B the Mo—Mo bond length is 2.70 Å as observed in our experiment. The bulk modulus of pure metal (Mo) is 272 GPa and that of Mo_2B is 302 GPa. The large decrease in the compressibility of the semiboride could be due to the presence of short B—B covalent bonds. Moreover, the intercalation of boron atoms in to TM atoms may be reason for higher bulk modulus.

3.2. Electronic properties

We now turn our attention to understand the basic electronic band structure, density of states and Fermi surface topology of Mo_2B at ambient conditions using FP-LAPW method. These calculations were performed using the optimized geometry at 0 GPa (See Table 1) obtained by VASP-PAW method. Fig. 5(a) shows the calculated band structure along with the high symmetry directions of the IBZ and corresponding density of states is presented in Fig. 6(a). From Fig. 5(a), it is identified that the bands are more

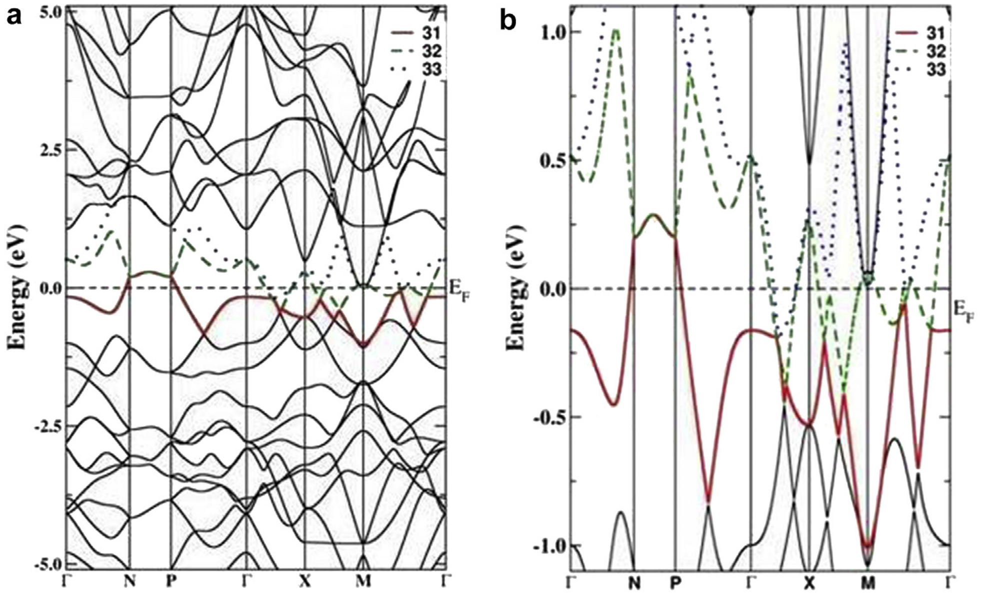

Fig. 5. Computed band structures of Mo_2B at ambient pressure using FP-LAPW method. Here the calculations are performed at optimized geometries obtained by VASP-PAW method.

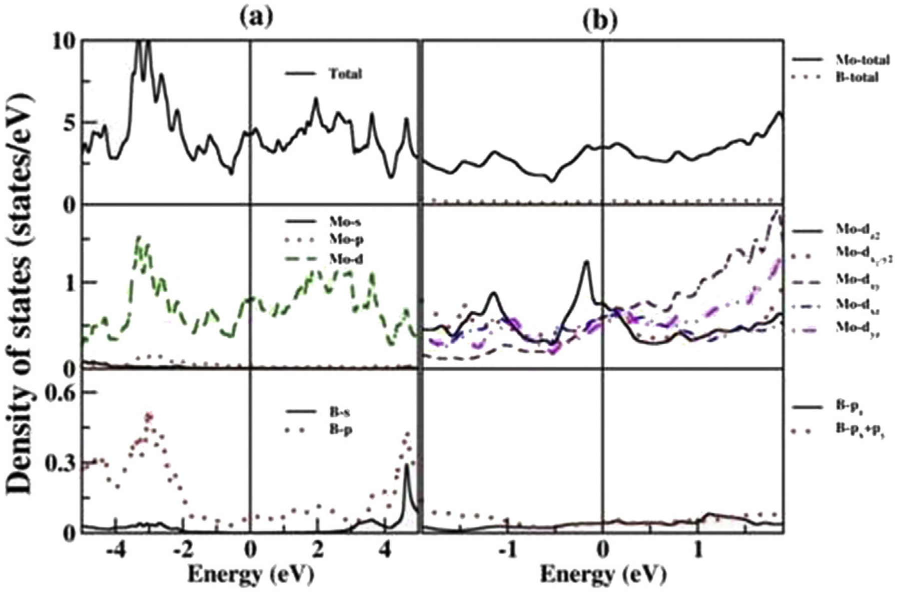

Fig. 6. Density of States of Mo_2B at ambient pressure using FP-LAPW method. Here the calculations are performed at optimized geometries obtained by VASP-PAW method.

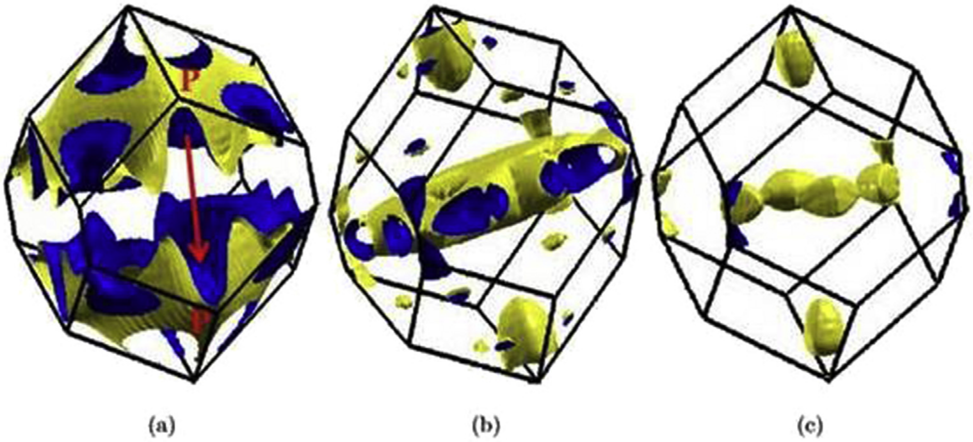

(a) (b) (c)

Fig. 7. Fermi surface of Mo_2B along with high symmetry points.

dispersive at the large energy scale regions (from −5 to −2 eV and 2–5 eV), and strongly hybridized with Mo (*d*) and B (*p*) – states. Furthermore, between the low energy ranges from −2 to 2 eV, Mo (*d*) states are largely predominant with very less contribution of B (*p*) states, which indicates Mo (*d*) – states to be strongest at the Fermi level. Three bands are crossing at the Fermi level (indicated with band numbers 31, 32, and 33); largely dominated with *d*-states of Mo atom and the respective band structure and density of states are shown in Fig. 5(b) and Fig. 6(b). It would be interesting to analyse the crystal field splitting of Mo-"*d*" states as one would expect a reasonable crystal field splitting of transition metal "d" states. To analyse this further, we have plotted the angular momentum projected density of states of Mo and B atoms and are shown in Fig. 6(b). It is quite evident that crystal field splitting of Mo "*d* " states is less predominant. The Fermi surfaces corresponding to the three bands crossing the Fermi level are presented in Fig. 7, where the band number 31 (Fig. 7(a)) indicating the hole nature of the band, cross the Fermi level along Γ- P, and Γ-N directions. The other two bands (32 and 33) are having electron nature and band number 32 cross the Fermi level along Γ - X, Γ-M, and X-M, while the other band 33 cross the Fermi level along Γ-X direction. The complicated Fermi surface corresponding to the bands 32 and 33 are shown in Fig. 7(b) and (c) respectively. Interestingly, we observed strong Fermi surface nesting along the P–P direction as seen in band 31 and the Fermi surface nesting and corresponding directions are shown in Fig. 7(a). Earlier, numerous studies have reported that combination of Fermi surface nesting and the Kohn anomaly in same high symmetry direction of phonon dispersion may lead to a sudden change in magnetic properties and anomalous lattice instability in several metals [18–26]. On the other hand, from the previous reports on phonon dispersion of Mo_2B, no such Kohn anomaly was identified in any of the q vector and hence it implies that the large dynamical instability at Γ point might be due to anharmonic effects. In addition, the strong Fermi surface nesting which is observed P–P direction may also bring about the lattice instability. The Fermi surface at 40 GPa is also presented, which still shows the nesting property as seen in Fig. 8. The present experiments indicate that Mo_2B is stable at room temperature and also up to the pressure of 40 GPa. This prompts us to state that temperature dependent calculations such as molecular

Fig. 8. Fermi surface of Mo_2B at high pressure (40 GPa).

dynamics or advanced statistical methods, which includes the anharmonic effects might be essential to address the theoretically observed lattice instability. In addition, the authors also emphasize that no reports were available on Fermi surface nesting for Mo_2B or any other transition metal semi borides until now and the present work may open up new insight and more understanding about this compound. In addition, high resolution angle resolved photoemission experiments are necessary for Mo_2B, enabling better understanding which can be taken up as the future work.

4. Conclusions

In summary, we have discussed HPXRD studies on transition semimetal boride Mo_2B up to a pressure of 40 GPa and the experimental results are compared with first principles calculations. The present experiment clearly demonstrated the ground state tetragonal structure with space group *I4/mcm* phase of Mo_2B to be stable upto the pressures we have studied. The experimentally observed quantities such as lattice parameters, volume and bulk modulii are complemented with the present theoretical calculations and also agree well with the previous reports. Similar to other Mo-based borides, Mo_2B also exhibits the ultra-incompressible nature. We have also performed the electronic band structure, density of states and Fermi surface calculations of Mo_2B using FP-LAPW method. We found strong Fermi surface nesting along P–P direction, which might be a possible reason for lattice instabilities observed by previous reports.

Acknowledgements

The authors thank N. R. Sanjay Kumar, B. Shukla and T. R. Ravindran for valuable discussions. They also thank IGCAR management for their support. G V and S A acknowledge CMSD, University of Hyderabad for providing computational facilities. V K acknowledge IITH for computational facility, G S acknowledge IITH for fellowship.

References

[1] A. Friedrich, B. Winkler, E.A. Juarez-Arellano, L. Bayarjargal, Synthesis of binary transition nitrides, carbides and borides from the elements in the laser heated diamond anvil cell and their structure-property relations, Materials 4 (2011) 1648–1692.